Journal of Organometallic Chemistry 694 (2009) 3793–3799

Contents lists available at ScienceDirect

Journal of Organometallic Chemistry

journal homepage: www.elsevier.com/locate/jorganchem

Synthesis and characterization of *para*-nitro substituted 2,6-bis(phenylimino) pyridyl Fe(II) and Co(II) complexes and their ethylene polymerization properties

Zerong Long [a,c], Biao Wu [a,b,*], Peiju Yang [a], Gang Li [a], Yanyan Liu [a,c], Xiao-Juan Yang [a,b]

[a] State Key Laboratory for Oxo Synthesis and Selective Oxidation, Lanzhou Institute of Chemical Physics, Chinese Academy of Sciences, Lanzhou 730000, China
[b] State Key Laboratory of Applied Organic Chemistry, Lanzhou University, Lanzhou 730000, China
[c] Graduate School of Chinese Academy of Sciences, Beijing 100049, China

ARTICLE INFO

Article history:
Received 17 November 2008
Received in revised form 8 July 2009
Accepted 14 July 2009
Available online 17 July 2009

Keywords:
Iron(II)
Cobalt(II)
2,6-bis(4-nitro-2,6-R_2-phenylimino)pyridines
Ethylene polymerization
Electronic effect

ABSTRACT

Four iron(II) and cobalt(II) complexes ligated by 2,6-bis(4-nitro-2,6-R_2-phenylimino)pyridines, $LMCl_2$ (**1**: R = Me, M = Fe; **2**: R = *i*Pr, M = Fe; **3**: R = Me, M = Co; **4:** R = *i*Pr, M = Co) have been synthesized and fully characterized, and their catalytic ethylene polymerization properties have been investigated. Among these complexes, the iron(II) pre-catalyst bearing the *ortho*-isopropyl groups (complex **2**) exhibited higher activities and produced higher molecular weight polymers than the other complexes in the presence of methylaluminoxane (MAO). A comparison of **2** with the reference non-nitro-substituted catalyst (2,6-bis(2,6-diisopropylphenylimino)pyridyl)$FeCl_2$ (FeCat **5**) revealed a modest increase of the catalytic activity and longer lifetime upon substitution of the *para*-positions with nitro groups (activity up to 6.0×10^3 kg mol^{-1} h^{-1} bar^{-1} for **2** and 4.8×10^3 kg mol^{-1} h^{-1} bar^{-1} for **5**), converting ethylene to highly linear polyethylenes with a unimodal molecular weight distribution around 456.4 kg mol^{-1}. However, the iron(II) pre-catalyst **1** on changing from *ortho*-isopropyl to methyl groups displayed much lower activities (over an order of magnitude) than **2** under mild conditions. As expected, the cobalt analogues showed relatively low polymerization activities.

1. Introduction

Since Brookhart [1] and Gibson [2] independently reported that 2,6-bis(phenylimino)pyridyl Fe(II) and Co(II) dihalide were highly effective catalysts for ethylene polymerization on treatment with methylaluminoxane (MAO), a great deal of interest has focused on the relationship between structure and activity of such catalysts [3–7]. It is generally thought that the steric and electronic effects of the ligand play a crucial role in the catalytic performance and polymer properties. The steric bulk of the *ortho*-substituents on the aryl rings, being close to the active site, is particularly important in ethylene polymerization/oligomerization. Studies have shown that a moderate increase of the size of the *ortho*-alkyl groups seemed to facilitate an increase of the productivity and the polymer molecular weight for the 2,6-bis(phenylimino)pyridyl iron(II) catalysts under mild reaction conditions [1–4]. When the iron(II) complex was substituted by a single alkyl group on one *ortho*-position, the catalyst showed either a rather low polymerization productivity and low polymer molecular weight (*M*w) or high ethylene oligomerization activities with an excellent selectivity of α-olefins (>95%) [2,8].

The catalytic activities of 2,6-bis(phenylimino)pyridyl iron and cobalt complexes can also be remarkably influenced by the electronic effect of the ligand substituents. It has been reported that iron or cobalt complexes with electronegative substituents (F, Cl, Br etc.) on both or single *ortho*-positions of the aryl rings displayed high activities for ethylene polymerization and/or oligomerization [5,6,9,10]. Introduction of electron-withdrawing groups (e.g. Br, F, CF_3 etc.) to the *para*-positions resulted in an increase of polymerization or oligomerization activities for such iron catalytic systems treated with MAO/MMAO, while steric effect appeared to be more dominant for cobalt catalysts [6,11–15]. Recently, Gibson and coworkers [16] reported a series of *para*-ferrocene-substituted bis(phenylimino)pyridyl iron(II) complexes which exhibited a modest increase of activity compared with the non-ferrocenyl iron catalysts due to the higher electrophilicity induced by the *para*-groups. There are also reports of palladium α-diimine complexes and iron(II) bis(imino)pyridyl complexes with strongly electron-withdrawing nitro groups. The former showed less activities and produced lower *M*w polymers, whereas the latter (iron catalysts incorporating two *para*-nitro substituents) displayed moderate thermal stabilities, longer lifetimes and lower oligomerization activities compared with the non-nitro-substituted systems [17,18]. In view of these results, it would be an effective approach

* Corresponding author. Address: State Key Laboratory for Oxo Synthesis and Selective Oxidation, Lanzhou Institute of Chemical Physics, Chinese Academy of Sciences, Lanzhou 730000, China. Tel./fax: +86 931 4968286.
E-mail address: wubiao@lzb.ac.cn (B. Wu).

0022-328X/$ - see front matter © 2009 Elsevier B.V. All rights reserved.
doi:10.1016/j.jorganchem.2009.07.027

to design bis(imino)pyridyl ligands with appropriate *ortho*-steric bulk and electron-withdrawing *para*-nitro-substituents for the purpose to achieve extended lifetimes and high activities for ethylene polymerization.

In the present work, we have designed two 2,6-bis(2,6-R_2-phenylimino)pyridyl ligands (R = CH_3 or *i*Pr) bearing strongly electron-withdrawing *para*-nitro substituents for the purpose of evaluating the electronic effect on the polymerization behavior of bis(imino)pyridine complexes. Herein we report the synthesis and characterization of the corresponding (2,6-bis(4-nitro-2,6-R_2-phenylimino)pyridyl)-$FeCl_2$ and -$CoCl_2$ complexes (**1**–**4**), as well as detailed studies of the effect of modification in ligand architecture (i.e. the steric and electronic properties) on the polymerization activities and the resultant polyolefins.

2. Results and discussion

2.1. Synthesis

Ligands $\mathbf{L^1}$ and $\mathbf{L^2}$ were prepared by the condensation of 2.2 equivalents of the corresponding nitroaniline with one equivalent of 2,6-diacetylpyridine (Scheme 1). When toluene was used as solvent according to traditional methods, a poor yield (6–10%) was obtained, perhaps due to the low basicity of nitroaniline [17]. Furthermore, prolonging reaction time (up to refluxing for 3 days) in cooperation with the use of molecular sieves to extract water could not improve the yield. Finally, we used tetraethyl silicate as solvent and water absorbent, and 2,6-bis(4-nitro-2,6-R_2-phenylimino)pyridines ($\mathbf{L^1}$ and $\mathbf{L^2}$, Scheme 1) were isolated in acceptable yields (33–55%).

Single crystals of $\mathbf{L^1}$ suitable for X-ray diffraction were obtained in dimethyl sulfoxide solution. The molecular structure of $\mathbf{L^1}$ (Fig. 1) reveals that the phenylimino groups are stretched away from the central pyridyl ring to release the steric constraints and are in the (E, E) conformation with typical C=N double bonds (1.279(2) and 1.271(2) Å) [6]. The two phenyl rings are nearly perpendicular to the pyridyl ring (dihedral angles 91.2° and 91.9°), while the nitro groups are approximately coplanar with the corresponding dimethylphenyl moiety (dihedral angle 4.0° and 12.5°, respectively).

The complexes **1**–**4** were prepared by reaction of equimolar $FeCl_2{\cdot}4H_2O$ or $CoCl_2{\cdot}6H_2O$ with the corresponding ligand in fleshly distilled THF or dichloromethane at room temperature, and were isolated as air-stable solids in moderate yield. They were characterized by elemental analysis, ESI–MS spectrometry and IR spectroscopy, which confirmed the composition $LMCl_2$ of the complexes. The IR spectra showed C=N stretching at 1648 cm^{-1} for the ligands and at 1614–1634 cm^{-1} for the complexes, indicating the coordination of the nitrogen atoms of phenylimino to the metal ions [3]. Complexes **2** and **4** were further characterized by X-ray crystallography.

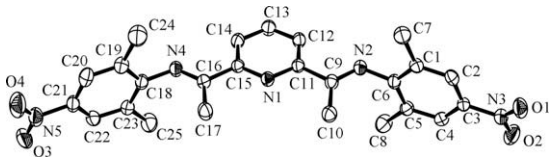

Fig. 1. Molecular structure of $\mathbf{L^1}$; hydrogen atoms are omitted for clarity. Selected bond lengths (Å) and angles (°): N4–C16 1.271(2), N2–C9 1.279(2), N4–C16–C15 116.7(2), N2–C9–C11 116.3(2), O3–N5–O4 123.5(2), O2–N3–O1 123.3(2).

The crystals of complex **2** were grown by slow diffusion of Et_2O into its THF-methanol solution under nitrogen atmosphere at room temperature. Complex **2** (Fig. 2) shows an approximate *Cs* symmetry about the plane defined by the iron atom, the two Cl atoms, and the pyridyl nitrogen atom. The geometry around the iron center can be described as a distorted square pyramid (τ value 0.45) [19] with a tridentate N^N^N ligand and two chlorides. The iron atom deviates ca. 0.54 Å from the plane of coordinated nitrogen atoms (N1, N2 and N3). The central Fe1–N1(Py) bond (2.093(4) Å) is significantly shorter than Fe1–N(imino) (2.250(4) and 2.251(4) Å). The Fe–Cl bonds (2.241(2) and 2.296(2) Å) in **2** are shorter than those (2.266(2) and 2.311(2) Å) in the known complex **5** [3], while the Fe–N bond lengths are slightly longer compared with those in **5** (2.088(4), 2.238(4) and 2.250(4) Å).

Complex **4** was crystallized by slow evaporation of its CH_2Cl_2-toluene solution at room temperature. The cobalt complex **4** (Fig. 3) is isomorphous to its iron analogue **2** with similar geometric characteristics. The deviation of the cobalt atom from the plane of its coordination nitrogen atoms is 0.55 Å. As in **2**, complex **4** has a five-coordinate, distorted square-pyramidal geometry around the Co(II) center with a τ value of 0.44. The Co–N(Py) bond (2.045(3) Å) in complex **4** is slightly shorter than that in (2,6-bis(2,6-diisopropylphenylimino)pyridyl)$CoCl_2$ (2.051(3) Å), yet the average Co–N(imino) bond length is comparable to that of the non-nitro Co(II) complex (Co–N, 2.211 Å). The Cl1–Co1–Cl2 bond angle (113.8(1)°) is slightly smaller than that in the latter compound (116.5°) [3].

2.2. Ethylene polymerization

The complexes **1**–**4** were used as pre-catalysts for ethylene polymerization. Upon treatment with MAO, all the complexes are active toward ethylene polymerization. Results of the polymerization reactions are listed in Tables 1 and 2 and Figs. 4 and 5.

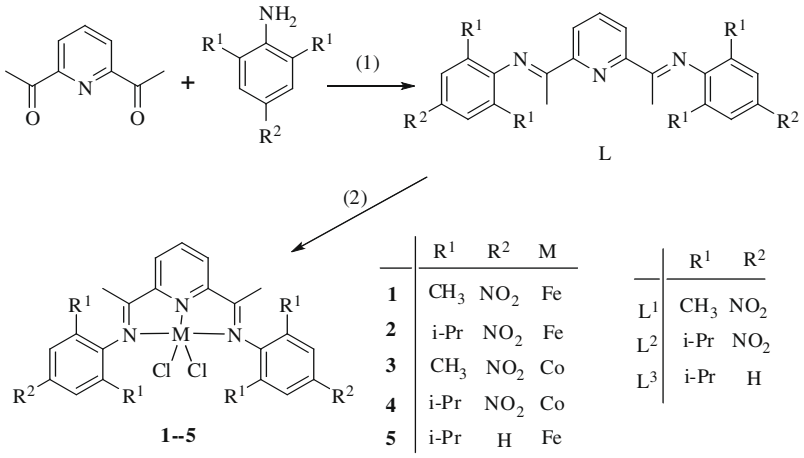

	R^1	R^2	M
1	CH_3	NO_2	Fe
2	i-Pr	NO_2	Fe
3	CH_3	NO_2	Co
4	i-Pr	NO_2	Co
5	i-Pr	H	Fe

	R^1	R^2
L^1	CH_3	NO_2
L^2	i-Pr	NO_2
L^3	i-Pr	H

Scheme 1. Synthesis of the ligands and complexes. Reagents and conditions: (1) *p*-toluenesulfonic acid, tetraethyl silicate; (2) $FeCl_2{\cdot}4H_2O$ or $CoCl_2{\cdot}6H_2O$, THF.

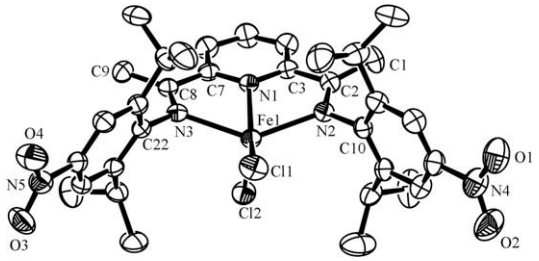

Fig. 2. Molecular structure of **2**. Hydrogen atoms and the crystalline methanol molecule are omitted for clarity. Selected bond lengths (Å) and angles (°): Fe1–N1 2.093(4), Fe1–N2 2.250(4), Fe1–N3 2.251(4), Fe1–Cl1 2.241(2), Fe1–Cl2 2.296(2), C2–N2 1.280(6), C8–N3 1.285(6), N1–Fe1–N2 73.0(2), N1–Fe1–N3 72.6(2), N2–Fe1–N3 140.3(2), N1–Fe1–Cl1 150.6(1), N1–Fe1–Cl2 94.8(1), N2–Fe1–Cl2 105.0(1), N2–Fe1–Cl1 100.2(1), N3–Fe1–Cl1 100.0(1), N3–Fe1–Cl2 97.1(1), Cl1–Fe1–Cl2 114.5(1).

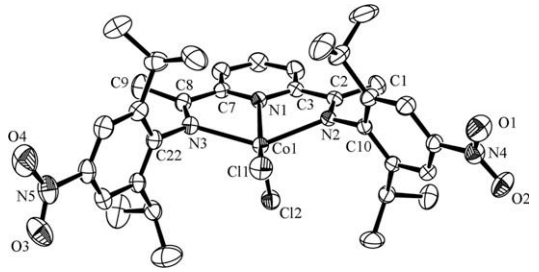

Fig. 3. Molecular structure of **4**. Hydrogen atoms and the crystalline CH_2Cl_2 molecule are omitted for clarity. Selected bond lengths (Å) and angles (°): Co1–N1 2.045(3), Co1–N2 2.208(3), Co1–N3 2.215(3), Co1–Cl1 2.217(2), Co1–Cl2 2.273(1), C2–N2 1.281(5), C8–N3 1.279(5), N1–Co1–N2 73.9(1), N1–Co1–N3 73.7(1), N2–Co1–N3 141.3(1), N1–Co1–Cl1 153.5(1), N1–Co1–Cl2 92.5(1), N2–Co1–Cl2 96.2(1), N2–Co1–Cl1 99.3(1), N3–Co1–Cl1 100.3(1), N3–Co1–Cl2 105.8(1), Cl1–Co1–Cl2 113.8(1).

2.2.1. Effect of the ligand environment and metal center

The precatalysts **2** and **5** have the same *ortho*-isopropyl groups on the aryl rings of the N^N^N tridentate ligand, and the difference between them is that the precatalyst **2** bears the strongly electron-withdrawing *para*-nitro substituents. Replacing the *para*-aryl protons with nitro groups (precatalyst **2**) resulted in a modest increase of the productivity and the molecular weight (*M*w) compared to **5**, from 4.8×10^3 to 6.0×10^3 kg mol^{-1} h^{-1} bar^{-1} and from 201.5 to 456.4 kg mol^{-1} respectively, and a decrease of the molecular weight distribution (MWD:*M*w/*M*n) from 37.8 to 21.0 (Table 1, runs 4, 9). Moreover, the precatalyst **2** showed a much higher productivity than the *ortho*-methyl analogue **1** (6.0×10^3 kg mol^{-1}

Table 2
Ethylene polymerization with complexes **2** and **5** in the presence of MAO.[a]

Run	Pre-catalyst	*T* (°C)	*t* (min)	PE (g)	Activity[b]
4	**2**	0	10	2.00	6.0
9	**5**	0	10	1.61	4.8
12	**2**	15	10	1.73	5.2
13	**5**	15	10	1.43	4.3
14	**2**	30	10	1.70	5.1
15	**5**	30	10	1.30	3.9
16	**2**	45	10	1.24	3.7
17	**5**	45	10	1.20	3.6
18	**2**	60	10	0.73	2.2
19	**5**	60	10	0.50	1.5
20	**2**	0	5	0.98	5.9
21	**5**	0	5	0.96	5.8
22	**2**	0	15	2.15	4.3
23	**5**	0	15	1.70	3.4
24	**2**	0	30	2.20	2.2
25	**5**	0	30	1.90	1.9
26	**2**	0	45	2.25	1.5
27	**5**	0	45	2.10	1.4
28	**2**	0	60	2.40	1.2
29	**5**	0	60	2.20	1.1

[a] Polymerization conditions: 2 μmol of pre-catalyst; 30 mL of toluene; ethylene of 1 bar; 2000 equiv of MAO.
[b] Polymers (103 kg mol^{-1} h^{-1} bar^{-1}).

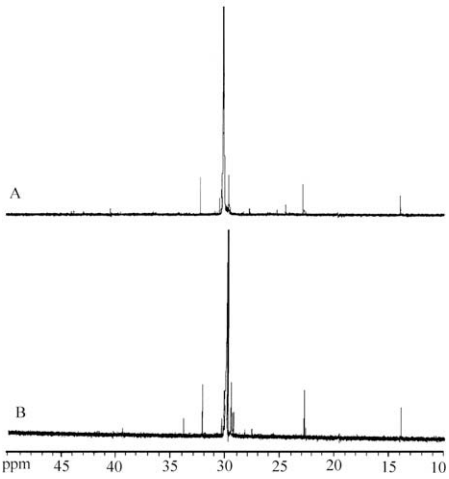

Fig. 4. ^{13}C NMR spectra (400 MHz, *o*-$C_6D_4Cl_2$, 135 °C) of the PEs produced by (A) complex **1**/MAO (run 1), and (B) complex **2**/MAO (run 4 in Table 1).

Table 1
Ethylene polymerization with complexes **1**–**5**.[a]

Run	Cat[b]	Al/M (mol/mol)	*t* (min)	Yield (g)	Activity[c]	Mn[d] kg/mol	*M*w[d] kg/mol	*M*w/*M*n[d]
1	**1**	2000	10	0.14	0.4	8.9	277.0	31.1
2	**2**	1000	10	0.64	1.9	27.5	645.9	23.4
3	**2**	1500	10	1.29	3.9	21.6	621.7	28.7
4	**2**	2000	10	2.00	6.0	21.7	456.4	21.0
5	**2**	2500	10	1.85	5.5	49.9	544.0	10.9
6	**2**	3000	10	1.71	5.1	41.4	458.5	11.1
7	**3**	2000	10	0.20	0.6	4.6	206.5	45.0
8	**4**	2000	10	0.31	0.9	11.8	286.7	24.3
9	**5**	2000	10	1.59	4.8	5.3	201.5	37.8
10[e]	**2**	2000	30	5.39	1.1	85.9	781.1	9.1
11[e]	**5**	2000	30	2.69	0.5	163.3	365.8	2.2

[a] Conditions: ethylene of 1 bar; reaction time: 10 min; reaction temperature: 0 °C; co-catalyst: MAO; solvent: 30 mL toluene.
[b] Pre-catalyst: 2 μmol.
[c] Polymers (103 kg mol^{-1} h^{-1} bar^{-1}).
[d] Determined by GPC.
[e] Ethylene of 5 bar, reaction temperature: 30–40 °C, 100 mL toluene.

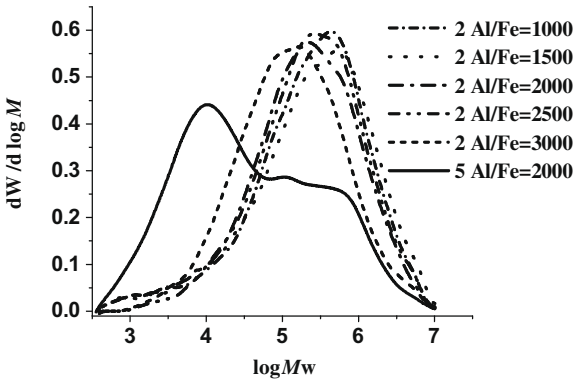

Fig. 5. GPC curves of the polymers prepared with pre-catalyst **2**/MAO (Al/Fe = 1000, 1500, 2000, 2500, 3000) and the reference pre-catalyst **5**/MAO (Al/Fe = 2000) at 0 °C, 1 bar ethylene for 10 min.

h^{-1} bar^{-1} for **2** and 0.4×10^3 kg mol^{-1} h^{-1} bar^{-1} for **1**) under the same reaction conditions, and the *M*w also dropped from 456.4 to 277.0 kg mol^{-1} (Table 1, runs 1, 4). It is likely that both the electronic effect and the steric bulk of the substituents caused the differences of the activities and polymer *M*w for these catalytic systems. With respect to the precatalyst **2** containing a more electron-withdrawing ligand, the electrophilic character on the center iron atom is enhanced remarkably, which makes the cationic species more active for ethylene insertion. Thus, the precatalyst **2** showed higher activities and produced higher molecular weight polyethylenes in comparison with the non-nitro substituted **5**. For the other factor, the ligand steric bulk, it is obvious that simply changing the size of the aryl *ortho*-substituents allows for control over both the catalyst activity and the polymer molecular weight [11], as has been reported for the non-nitro substituted iron catalytic system on changing from 2,6-diisopropyl (1.1×10^3 kg mol^{-1} h^{-1} bar^{-1}, 203.0 kg mol^{-1}) to 2,6-dimethyl groups (0.6×10^3 kg mol^{-1} h^{-1} bar^{-1}, 29.0 kg mol^{-1}) upon activation with MAO [2]. This is in line with the behavior of the nitro-substituted derivatives in the present work, where the precatalyst **2** has a higher polymer activity and higher *M*w than **1** for the distinction of their steric protection toward the active center.

In the cases of the cobalt complexes **3** and **4**, the *ortho*-isopropyl derivative **4** also showed a slightly higher activity (0.9×10^3 kg mol^{-1} h^{-1} bar^{-1}) and polymer *M*w (286.7 kg mol^{-1}) than the methyl derivative **3** (0.6×10^3 kg mol^{-1} h^{-1} bar^{-1}, 206.5 kg mol^{-1}), although their activities are much lower than those of the corresponding iron analogues. It has been reported that non-nitro substituted cobalt catalytic system displayed a slight increase in polymer activity and a decrease in *M*w on changing from *ortho*-isopropyl (0.7×10^3 kg mol^{-1} h^{-1} bar^{-1}, 43.0 kg mol^{-1}) to *ortho*-methyl groups (0.9×10^3 kg mol^{-1} h^{-1} bar^{-1}, 3.7 kg mol^{-1}) with treatment of MMAO [1], which is slightly different from the nitro-substituted derivatives upon activation with MAO in this work (Table 1, runs 7 and 8). For the cobalt system, introduction of *para*-nitro groups on the aryl rings had no evident effect on the polymer activities but remarkably improved the polymer mass. On the other hand, the polymers produced by the cobalt(II) complexes have lower molecular weights and slightly broader molecular weight distributions (*M*w/*M*n) compared with the iron analogues. This could be attributed to the different inherent electronic properties of Fe and Co that led to distinction in chain propagation and chain transfer rates of the two systems [3].

The polyethylenes (PEs) produced by catalysts **1** and **2** were analyzed by ^{13}C NMR spectroscopy (Fig. 4), which revealed that the precatalyst **1** yielded PEs with small amounts of methyl ends (δ = 14.0 ppm) and isopropyl chain ends (δ = 24.4 and 28.2 ppm) (Fig. 4A). However, no detectable unsaturated groups for the polymers produced by the precatalyst **1** were observed, probably due to the chain transfer to aluminum which resulted in almost completely saturated polymer chains. The polymers obtained by **1** are highly linear and only one methyl branch per 1000 carbon atoms can be observed. The PEs produced by the precatalyst **2** are also highly linear with saturated methyl ends and a 1:3 ratio of unsaturated (1.3 per 1000 C) to saturated end groups, and almost no branch is observed (Fig. 4B). These results are consistent with the polymers produced by the non-nitro substituted iron-based precatalysts, in which saturated end groups are much more than unsaturated end groups involving a combination of chain transfer to aluminum and β-H transfer [3]. The facts that the precatalyst **1** and **2** produced exclusively high molecular weight and highly linear polyethylenes may suggest that the *para*-nitro substituted 2,6-bis(phenylimino)pyridyl ligands could restrain the active iron center from deactivation and chain transfer reactions.

2.2.2. Effects of the reaction conditions

The effects of the concentration of MAO, reaction time and temperature, ethylene pressure, and especially the ligand architecture on the polymerization activities and product properties of pre-catalyst **2** have been investigated. To examine the role of the MAO in the polymerization, the molar ratio of Al/Fe was varied from 1000 to 3000. As shown in Table 1, the productivity of **2** increased with increasing Al/Fe ratio, reaching a maximum at Al/Fe = 2000, and then decreased slightly with more MAO (Al/Fe up to 3000) at 0 °C (Table 1, runs 2–6). The molecular weight (*M*w) and MWD of the products showed a decreasing trend with increasing Al/Fe ratio. Fig. 5 shows the GPC traces of a series of polymerization tests of precatalysts **2** and **5**. When the ratio of Al/Fe is 1000, a broad unimodal molecular weight distribution is observed, with an M_{pk} at 500 kg mol^{-1} for precatalyst **2**. A similar broad unimodal molecular weight distribution was also found at other Al/Fe ratios for precatalyst **2**, and the value of M_{pk} decreased with increasing Al/Fe ratio (1500, 400; 2000, 280; 2500, 250 and 3000, 125 kg mol^{-1}). However, with 2000 equiv of MAO a broad distribution is observed with an M_{pk} at 10 kg mol^{-1} and a broader shoulder in the range 100–600 kg mol^{-1} for the non-nitro substituted **5**. A bimodal molecular weight distribution has been commonly observed for iron catalysts with increasing MAO concentrations [9]; however, the unimodal molecular weight distribution has been obtained in the *para*-nitro substituted precatalyst **2** as well as in bis(phenylimino)pyridine·$FeCl_2$ with ω-allyloxy substituents on the 4-position of the pyridyl ring for less chain transfer reactions [20].

The polymerization time and reaction temperature were also considered in evaluating the activity of pre-catalyst **2** (Table 2). At 1 bar of ethylene, the high catalytic activity of the complex **2** was found to persist for up to 10 min, followed by a laggard attenuation. Although the initial activity of the FeCat **5** was rather close to that of complex **2**, a rapid deactivation was observed over 5 min. Hence, the pre-catalyst **2** displayed a much higher average polymerization activity than **5** (Table 2, runs 4, 9, 20–29). The high polymer activity of the precatalyst **2** might be attributed to the electron-withdrawing nature of the nitro substituents, which results in a more electrophilic iron center in the complex, and thus increases the corresponding activity in ethylene polymerization. On the other hand, although nitro-substituted **2** has slightly longer lifetime than the non-nitro substituted **5**, deactivation soon occurred with more than 10 min. The reason might be that side reactions involving reduction of the nitro group have taken place in a prolonged reaction time, resulting in the loss of productivity. As proved by IR spectroscopy, the strong stretching of the nitro group in the precatalysts weakened significantly after interaction with an excess of MAO for 15 min. Similar deactivations were also ob-

served in related nitro-substituted bis(phenylimino)pyridyl iron(II) complexes applied in the oligomerization of ethylene [17].

The effect of reaction temperature on the catalytic activity is remarkable since polymerization is an exothermic process. A series of experiments were carried out to determine the effect of temperature variation on the catalyst performance. Table 2 shows the polymerization results at 0, 15, 30, 45 and 60 °C, respectively, employing pre-catalysts **2** and **5** at 1 bar. A significant reduction of the productivity was obtained at elevated temperatures for both precatalysts **2** and **5**, which is probably due to potential decomposition of the pre-catalysts **2** and **5** at higher temperature.

Polymerization pressure is another significant factor that influences the activities of the catalysts and molecular weight distribution of the polymers [3]. At 5 bar ethylene pressure, the complex **2** showed lower polymerization activities and narrower molecular weight distributions (Table 1, run 10) than those observed at 1 bar ethylene pressure due to the increase of both rate constants of chain propagation and β-H transfer at higher pressure, which were responsible for high molecular weights and narrower molecular weight distributions [3]. Although the catalytic activity of the complex **2** seemed to precede over complex **5**, lower molecular weight and narrower distribution polymers (Mw: 365.8 kg mol^{-1}; MWD: 2.2) were observed for **5** under same reaction conditions (Table 1, runs 10 and 11). It is obvious that the polymerization properties are strongly dependent on the electronic feature of the ligand.

3. Conclusions

Four iron(II) and cobalt(II) complexes ligated by 2,6-bis(4-nitro-2,6-R$_2$-phenylimino)pyridines have been synthesized, which are active ethylene polymerization catalysts in the presence of MAO. The iron pre-catalyst **2** displayed moderately increased catalytic activities relative to the non-nitro substituted analogue **5**, which was ascribed to the strongly electron-withdrawing *para*-nitro groups that can increase the Lewis acidic character of the iron cationic center. The *ortho* steric effect in such iron catalytic systems also played a significant role in controlling the catalyst activity and polymer mass, as complex **1** with *ortho*-methyl substituents on the aryl rings showed much lower polymerization activities than the *ortho*-isopropyl analogue **2**. The iron pre-catalysts **1**/MAO and **2**/MAO produced linear, high molecular weight polymers with a rather low embranchment, while the cobalt precatalysts **3** and **4** showed low activities and low Mw products by treating with MAO.

4. Experimental

4.1. General

All synthetic manipulations were carried out under a nitrogen atmosphere using standard Schlenk and cannula techniques. The NMR data of the polyethylenes were obtained on a Varian Unity-400 MHz spectrometer at 135 °C, with o-$C_6D_4Cl_2$ as solvent. The NMR spectra of the ligands were recorded on a Mercury plus-400 spectrometer at ambient temperature in $CDCl_3$. Elementary analyses were performed on a VarioEL instrument from Elementar Analysensysteme GmbH. IR spectra were measured with an HP5890II GC/NEXUS870. ESI-MS measurements were carried out with a Waters ZQ-4000 instrument (Waters, Manchester, UK). Weight-average (Mw), molecular weight distribution (Mw/Mn) were measured by a Waters gel permeation chromatograph Alliance GPCV 2000 at 150 °C using 1,2,4-trichlorobenzene as the eluent. Solvents were refluxed over an appropriate drying agent and distilled under nitrogen prior to use. MAO (10% solution in toluene) was purchased from Albemarle Corp. (USA). All other chemicals were purchased from commercial resources and used without further purification. 2,6-Dimethyl-4-nitroaniline, 2,6-diisopropyl-4-nitroaniline [21,22] and 2,6-diacetylpyridine(2,6-diisopropylanil)$FeCl_2$ were prepared by established procedures [3].

4.2. Synthesis of the ligands

4.2.1. 2,6-Dimethyl-4-nitroanil-2,6-diactylpyridine (**L^1**)

2,6-Dimethyl-4-nitroaniline (730.7 mg, 4.4 mmol) was added to a solution of 2,6-diactylpyridine (326.3 mg, 2.0 mmol) with a catalytic amount of p-toluenesulfonic acid (20.0 mg, 0.1 mmol) in tetraethyl silicate (1 mL)/toluene (20 mL) under nitrogen atmosphere. The mixture was refluxed for 3 days under nitrogen until no reactant 2,6-diactylpyridine remained. The solvents were evaporated under reduced pressure and the yellow solid was subsequently purified by column chromatography on silica gel with light petroleum ether/EtOAc (5:1) as the eluent. The yellow solid thus obtained was recrystallized by dichloromethane/light petroleum ether (1:5) to give a pale-yellow solid (301.7 mg, 33%). Mp: 299–300 °C. IR (KBr, cm^{-1}): 2912, 1648 (s, $\nu_{C=N}$, imine), 1588, 1505, 1328, 1214, 1098, 900, 775, 748, 711, 625. ^{1}H NMR (400 MHz, $CDCl_3$, ppm): 8.50 (d, J = 16 Hz, 2H, Py-H$_m$), 8.06 (s, 4H, Ar-H), 7.91 (t, 1H, Py-H$_p$), 2.28 (s, 6H, N=C-CH$_3$), 2.14 (s, 12H, Ar-CH$_3$). ^{13}C NMR (100.6 MHz, $CDCl_3$, ppm): 167.3 (C=N), 154.7 (Py-C$_o$), 154.3 (Ar-N=*C*), 143.5 (Ar-*C*-NO$_2$), 137.3 (Ar-*C*-Me), 126.6 (Py-C$_p$), 123.5 (Py-C$_m$), 123.0 (Ar-C$_m$), 18.0 (C=N-*C*H$_3$), 17.1 (Ar-*C*H$_3$). ESI–MS: m/z 460.5 [M+H]$^+$. Anal. Calc. for $C_{25}H_{25}N_5O_4$: N, 15.24; C, 65.35; H, 5.48. Found: N, 15.18; C, 65.15; H, 5.35%.

4.2.2. 2,6-Diisopropyl-4-nitroanil-2,6-diactylpyridine (**L^2**)

2,6-Diisopropyl-4-nitroaniline (978.0 mg, 4.4 mmol) was added to a solution of 2,6-diactylprydine (326.3 mg, 2.0 mmol) with a catalytic amount of p-toluenesulfonic acid (20.0 mg, 0.1 mmol) in tetraethyl silicate (5 mL) under nitrogen atmosphere. The mixture was stirred at 125 °C for 12 h. The solvent was evaporated under reduced pressure, and the residue was subsequently purified by column chromatography (silica gel; eluting reagent light petroleum/EtOAc (4:1)) to yield a yellow solid (628.9 mg, 55%). Mp: >300 °C. IR (KBr, cm^{-1}): 2911, 1648 (s, $\nu_{C=N}$), 1588, 1504, 1328, 1213,1097, 900, 775, 748, 625. ^{1}H NMR (400 MHz, $CDCl_3$, ppm): 8.49 (d, J = 10.8 Hz, 2H, Py–H$_m$), 8.08 (s, 4H, Ar–H), 8.00 (t, 1H, Py–H$_p$), 2.79 (m, 4H, C*H*(CH$_3$)$_2$), 2.30 (s, 6H, N=C–CH$_3$), 1.21 (m, 24H, CH(C*H*$_3$)$_2$). ^{13}C NMR (100.6 MHz, $CDCl_3$, ppm): 167.0 (C=N), 154.3 (Py–C$_o$), 152.4 (Ar–*C*-N=C), 144.6 (Ar-*C*-NO$_2$), 137.4 (Ar-*C*-Me), 137.2 (Py-C$_p$), 123.0 (Py-C$_m$), 119.3 (Ar-C$_m$), 29.7 (C=N-*C*H$_3$), 23.7 (*C*H(CH$_3$)$_2$), 17.6 (CH(*C*H$_3$)$_2$). ESI–MS: m/z 572.6 [M+H]$^+$. Anal. Calc. for $C_{33}H_{41}N_5O_4$: N, 12.25; C, 69.33; H, 7.23. Found: N, 12.00; C, 69.33; H, 7.17.

4.3. Synthesis of the complexes

1: A mixture of $FeCl_2{\cdot}4H_2O$ (38.8 mg, 0.20 mmol) with **L^1** (89.6 mg, 0.2 mmol) in freshly distilled THF (5 mL) was stirred at room temperature for 24 h. The dark precipitate formed was filtered and washed with THF (2 × 2 mL) and freshly distilled diethyl ether (2 × 5 mL). After dried in vacuum, the iron(II) complex **1** was obtained as a gray powder (yield: 78.2 mg, 67%). Mp: >300 °C. IR (KBr, cm^{-1}): 3090, 2962, 2917, 2852, 1634 (w, $\nu_{C=N}$), 1588, 1515, 1468, 1437, 1340, 1260, 1217, 1102, 891, 816, 779, 745, 454. Anal. Calc. for $C_{25}H_{25}Cl_2FeN_5O_4$: N, 11.95; C, 51.22; H, 4.30. Found: N, 11.64; C, 50.81; H, 4.02%. ESI–MS: m/z 551.5 [M–Cl]$^+$, 258.1 [M–2Cl]$^{2+}$.

2: In a similar manner to that described for **1**, the iron complex **2** was prepared as a dark cyan powder (60.1 mg, 43%). Mp: >300 °C.

Table 3
Crystal data and structure refinement for $\mathbf{L^1}$, **2**, and **4**.

	$\mathbf{L^1}$	**2**·CH_3OH	**4**·CH_2Cl_2
Formula	$C_{25}H_{25}N_5O_4$	$C_{34}H_{45}Cl_2FeN_5O_5$	$C_{34}H_{43}Cl_4CoN_5O_4$
Fw	459.50	730.50	786.46
Crystal system	monoclinic	monoclinic	monoclinic
Space group	*P*2(1)/*c*	*P*2(1)/*n*	*P*2(1)/*n*
a (Å)	8.5098(5)	9.0052(6)	9.005(2)
b (Å)	17.060(1)	30.556(2)	28.401(6)
c (Å)	16.460(1)	14.855(1)	15.018(3)
β (°)	91.896(3)	94.910(3)	93.57(3)
V (Å)	2388.3(3)	4072.7(4)	3833.3(13)
Z	4	4	4
D_{calc}/g cm^{-3}	1.278	1.191	1.363
crystal size (mm)	0.29 × 0.17 × 0.10	0.30 × 0.12 × 0.04	0.45 × 0.15 × 0.14
θ range (°)	1.72–26.77	1.92–25.06	1.43–25.06
Reflns collected/unique	14001/5069 [R_{int} = 0.0378]	21095/7199 [R_{int} = 0.0664]	12231/6674 [R_{int} = 0.0319]
Data/restraints/parameters	5069/0/307	7199/1/424	6674/2/433
Absorption coefficient (mm^{-1})	0.089	0.543	0.769
F(0 0 0)	968	1536	1636
*R*1; *wR*2 [(*I*) > 2*σ*(*I*)]	0.0511; 0.1239	0.0755; 0.2181	0.0645; 0.1803
*R*1; *wR*2 (all data)	0.0900; 0.1469	0.1348; 0.2628	0.0736; 0.1920
GOF	1.019	1.040	1.120

IR (KBr, cm^{-1}): 3084, 2965, 2927, 2869, 1614 (w, $\nu_{C=N}$), 1582, 1525, 1462, 1438, 1348, 1325, 1264, 1217, 1102, 1032, 939, 891, 779, 454. Anal. Calc. for $C_{33}H_{41}Cl_2FeN_5O_4$?CH_3OH: N, 9.59; C, 55.90; H, 6.21. Found: N, 9.89; C, 55.43; H, 6.02%. ESI–MS: *m/z* 664.5 [M–Cl]$^+$, 314.2 [M–2Cl]$^{2+}$.

3: In a similar manner to that described for **1**, the cobalt complex **3** was prepared as a green–yellow powder (83.7 mg, 71%). Mp: >300 °C. IR (KBr, cm^{-1}): 2956, 2920, 2852, 1626 (w, $\nu_{C=N}$), 1589, 1519, 1469, 1340, 1261, 1216, 1101, 1028, 940, 893, 815, 779, 745, 454. Anal. Calc. for $C_{25}H_{25}Cl_2CoN_5O_4$·0.5THF: N, 11.20; C, 51.85; H, 4.67. Found: N, 10.77; C, 51.69; H, 4.58%. ESI–MS: m/z 553.5 [M–Cl]$^+$, 259.3 [M–2Cl]$^{2+}$.

4: In a similar manner to that described for **1**, the cobalt complex **4** was prepared as a yellow powder (65.9 mg, 47%). Mp: >300 °C. IR (KBr, cm^{-1}): 2966, 2922, 2852, 1625 (w, $\nu_{C=N}$), 1586, 1521, 1463, 1349, 1326, 1262, 1212, 1099, 1075, 1025, 900, 739, 448. Anal. Calc. for $C_{33}H_{41}Cl_2CoN_5O_4$: N, 9.98; C, 56.50; H, 5.89. Found: N, 9.55; C, 56.07; H, 5.67%. ESI–MS: *m/z* 665.7 [M–Cl]$^+$, 315.6 [M–2Cl]$^{2+}$.

4.4. X-ray crystallography

Diffraction data for crystals of $\mathbf{L^1}$, **2** and **4** were collected on a Bruker SMART APEX II diffractometer with graphite-monochromated Mo Kα radiation (*λ* = 0.71073 Å) at 293(2) K. Intensities were corrected for empirical absorption [23]. The structures were solved by direct methods and refined by full-matrix least squares on F^2. All non-hydrogen atoms were refined anisotropically. All hydrogen atoms were placed in calculated positions. Structure solutions were performed by using the SHELXL-97 package [24]. The crystal data collections and refinement details for ligand $\mathbf{L^1}$ and complexes **2** and **4** are summarized in Table 3.

4.5. Procedure for ethylene polymerization

4.5.1. Ethylene polymerization at ambient pressure

The pre-catalyst (2 μmol) was added to a Schlenk flask under nitrogen atmosphere. The Schlenk flask was evacuated and then filled with nitrogen, and charged with 30 mL of fleshly distilled toluene. The mixture was stirred intensively for 5 min at setting temperature. The required amount of MAO was subsequently added via a syringe, and the reaction solution was stirred for desired period of time under ethylene (1 bar). The polymerization was terminated with acidified ethanol. The solid polyethylene was filtered, washed with ethanol, and dried in vacuum oven at 60 °C overnight. The polymer was characterized by GPC and ^{13}C NMR.

4.5.2. Ethylene polymerization at elevated pressure

The ethylene polymerization at elevated pressure was performed in a stainless autoclave (500 mL). The complex (2 μmol) and the required amount of MAO were dissolved in 100 mL of fleshly distilled toluene under nitrogen atmosphere, and the solution was subsequently transferred to the reactor via a syringe. The reaction mixture was stirred for the desired time under corresponding pressure of ethylene. The reaction was terminated and analyzed by using the same method as described above for the reaction with 1 bar ethylene.

Acknowledgements

This work was supported by the "Bairen Jihua" project of the Chinese Academy of Sciences.

Appendix A. Supplementary material

CCDC 726170 contains the supplementary crystallographic data for this paper. These data can be obtained free of charge from The Cambridge Crystallographic Data Centre via www.ccdc.cam.ac.uk/data_request/cif. Supplementary data associated with this article can be found, in the online version, at doi:10.1016/j.jorganchem.2009.07.027.

References

[1] B.L. Small, M. Brookhart, A.M.A. Bennett, J. Am. Chem. Soc. 120 (1998) 4049.
[2] G.J.P. Britovsek, V.C. Gibson, B.S. Kimberley, P.J. Maddox, S.J. McTavish, G.A. Solan, A.J.P. White, D.J. Williams, Chem. Commun. (1998) 849.
[3] G.J.P. Britovsek, M. Bruce, V.C. Gibson, B.S. Kimberley, P.J. Maddox, S. Mastroianni, S.J. McTavish, C. Redshaw, G.A. Solan, S. Strömberg, A.J.P. White, D.J. Williams, J. Am. Chem. Soc. 121 (1999) 8728.
[4] G.J.P. Britovsek, S. Mastroianni, G.A. Solan, S.P.D. Baugh, C. Redshaw, V.C. Gibson, A.J.P. White, D.J. Williams, M.R.J. Elsegood, Chem. Eur. J. 6 (2000) 2221.
[5] Y. Chen, C. Qian, J. Sun, Organometallics 22 (2003) 1231.
[6] Y. Chen, R. Chen, C. Qian, X. Dong, J. Sun, Organometallics 22 (2003) 4312.
[7] A.S. Abu-Surrah, L. Kristian, U. Piironen, P. Lehmus, T. Repo, M. Leskelä, A.J.P. White, D.J. Williams, J. Organomet. Chem. 648 (2002) 55.
[8] B.L. Small, M. Brookhart, J. Am. Chem. Soc. 120 (1998) 7143.
[9] K.P. Tellmann, V.C. Gibson, A.J.P. White, D.J. Williams, Organometallics 24 (2005) 280.

[10] Z. Zhang, S. Chen, X. Zhang, H. Li, Y. Ke, Y. Lu, Y. Hu, J. Mol. Catal. A: Chem. 230 (2005) 1.
[11] (a) V.C. Gibson, C. Redshaw, G.A. Solan, Chem. Rev. 107 (2007) 1745;
(b) C. Bianchini, G. Giambastiani, I.G. Rios, G. Mantovani, A. Meli, A.M. Segarra, Coord. Chem. Rev. 250 (2006) 1391.
[12] F. Pelascini, F. Peruch, P.J. Lutz, M. Wesolek, J. Kress, Eur. Polym. J. 41 (2005) 1288.
[13] I.S. Paulino, U. Schuchardt, J. Mol. Catal. A: Chem. 211 (2004) 55.
[14] J.-Y. Liu, Y. Zheng, Y.-G. Li, L. Pan, Y.-S. Li, N.-H. Hu, J. Organomet. Chem. 690 (2005) 1233.
[15] M.E. Bluhm, C. Folli, M. Döring, J. Mol. Catal. A: Chem. 212 (2004) 13.
[16] V.C. Gibson, N.J. Long, P.J. Oxford, A.J.P. White, D.J. Williams, Organometallics 25 (2006) 1932.
[17] A.S. Ionkin, W.J. Marshall, D.J. Adelman, A.L. Shoe, R.E. Spence, T. Xie, J. Polym. Sci. Part A: Polym. Chem. 44 (2006) 2615.
[18] C. Popeney, Z. Guan, Organometallics 24 (2005) 1145.
[19] A.W. Addison, T.N. Rao, J. Reedijk, J.van. Rijn, G.C. Verschoor, J. Chem. Soc. Dalton Trans. (1984) 1349.
[20] M. Seitz, W. Milius, H.G. Alt, J. Mol. Catal. A: Chem. 261 (2007) 246.
[21] W.A. Denny, G.J. Atwell, B.C. Baguley, J. Med. Chem. 26 (1983) 1625.
[22] F.J. Carver, C.A. Hunter, D.J. Livingstone, J.F. McCabe, E.M. Seward, Chem. Eur. J. 8 (2002) 2847.
[23] G.M. Sheldrick, Program SADABS: Area-Detector Absorption Correction, University of Göttingen, Germany, 1996.
[24] G.M. Sheldrick, SHELXS-97, SHELXL-97, Programs for Crystal Structure Analysis, University of Göttingen, Germany, 1997.